Comptes Rendus
Chimie
Supplementary material to the article available at:
https://doi.org/10.5802/crchim.223

Supplementary material: An efficient transition-metal-free route to oligo-α-pyridylamines via fluoroarenes

Alessio Nicolini [*, a], **Biagio Anderlini** [a], **Fabrizio Roncaglia** [a] **and Andrea Cornia** [*, a]

[a] Department of Chemical and Geological Sciences, University of Modena and Reggio Emilia & INSTM, I-41125 Modena, Italy

E-mails: alessio.nicolini@unimore.it (A. Nicolini), biagio.anderlini@unimore.it (B. Anderlini), fabrizio.roncaglia@unimore.it (F. Roncaglia), acornia@unimore.it (A. Cornia)

Scheme S1: Synthesis of H_3py_3tren.
(1) Synthesis of HBrdpa.
(2) ^{1}H NMR spectrum of HBrdpa (Figure S1).
(3) 2D NMR spectra of HFdpa (Figures S2–S4).
(4) 2D NMR spectra of $H_6tren(dpa)_3$ (Figures S5–S8).
(5) Details on ^{1}H NMR and ESI-MS detection of **SPa** (Figures S9 and S10, Scheme S2).

* Corresponding authors.

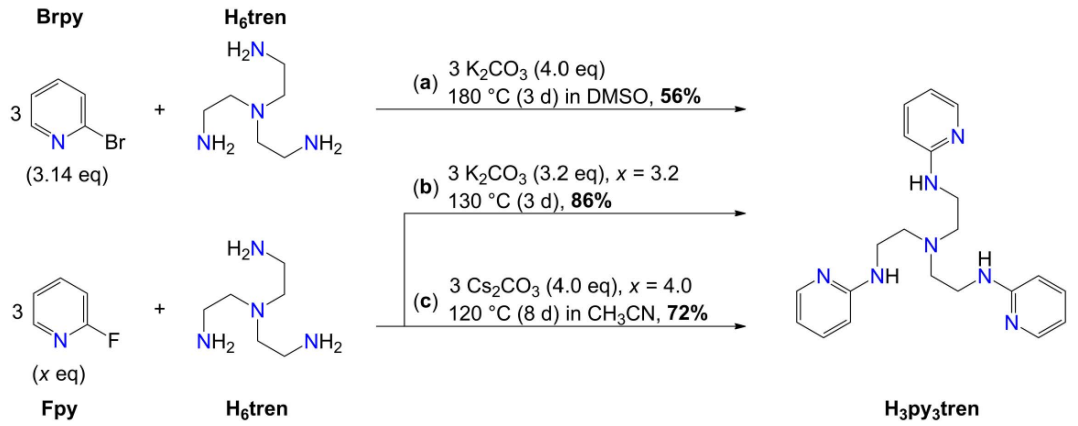

Scheme S1. Synthesis of H_3py_3tren as described in Ref. [1] (a), Ref. [2] (b), and Ref. [3] (c), with quoted isolated yields.

(1) Synthesis of HBrdpa

In a three neck round bottom flask (1 L) equipped with a mechanical overhead stirrer and a condenser, NH_2py (5.2510 g, 55.796 mmol) and Br_2py (13.2155 g, 55.787 mmol) were dissolved in anhydrous toluene (500 mL) under nitrogen atmosphere. ^{t}BuOK (10.2110 g, 90.999 mmol) was carefully added to the pale-yellow solution, which progressively turned to dark blue/black. The reaction mixture was heated to 80 °C and vigorously stirred for three days. It is worth to note that a mechanical stirrer is essential as a very dense solid mass is formed at a temperature of about 70 °C during the initial heating. This solid is progressively dispersed into the liquid phase during the first 24 h of reaction time. The reaction was monitored through thin-layer chromatography (TLC) on silica gel plates (one drop of reaction mixture in 0.5 mL of CH_2Cl_2; eluent Et_2O:*n*-hexane, 1:1 v/v; $R_f(NH_2py) = 0.02$; R_f(HBrdpa) = 0.31; $R_f(Br_2py) = 0.55$) and ^{1}H NMR spectroscopy in deuterated dimethyl sulfoxide (DMSO-d_6). The suspension was allowed to cool to room temperature, and the solvent was evaporated under reduced pressure. The light-pink solid obtained was dissolved in CH_2Cl_2 (300 mL) and washed with water (150 mL+2×50 mL). The inorganic phases were extracted with CH_2Cl_2 (2 × 50 mL). The organic phases were combined and dried over $MgSO_4$ (90 min). The desiccant was filtered off and the red organic solution was evaporated to dryness, to give a dark orange oil which slowly crystallized under vacuum (~14.0 g). This crude product was purified through gradient-elution FC (for ~7 g of crude material: SiO_2; eluent petroleum ether:Et_2O, from 1:0 to 1:1 v/v; $t_{gradient}$ = 25 min, flow rate = 40 mL/min, column diameter = 40 mm, column length = 150 mm), which gave HBrdpa as a pale-yellow solid (9.01 g, 36.0 mmol, 64.6% isolated yield).

Mp 87.7–88.4 °C. ^{1}H NMR (DMSO-d_6, 298 K, 400.13 MHz): δ_H (ppm) = 10.03 (1H, s, H*h*), 8.24 (1H, ddd, $^3J(a,b) = 5.0$, $^4J(a,c) = 1.9$, $^5J(a,d) = 0.8$, H*a*), 7.92 (1H, dd, $^3J(g,f) = 8.3$, $^4J(g,e) = 0.4$, H*g*), 7.69 (1H, ddd, $^3J(c,d) = 8.4$, $^3J(c,b) = 7.2$, $^4J(c,a) = 2.0$, H*c*), 7.59 (1H, pt, $^3J(f,e) \sim {}^3J(f,g) \sim 7.9$, H*f*), 7.48 (1H, dpt, $^3J(d,c) = 8.4$, $^4J(d,b) \sim {}^5J(d,a) \sim 0.9$, H*d*), 7.06 (1H, dd, $^3J(e,f) = 7.5$, $^4J(e,g) = 0.5$, H*e*), 6.91 (1H, ddd, $^3J(b,c) = 7.2$, $^3J(b,a) = 5.0$, $^4J(b,d) = 1.0$, H*b*).

(2) ^{1}H NMR spectrum of HBrdpa

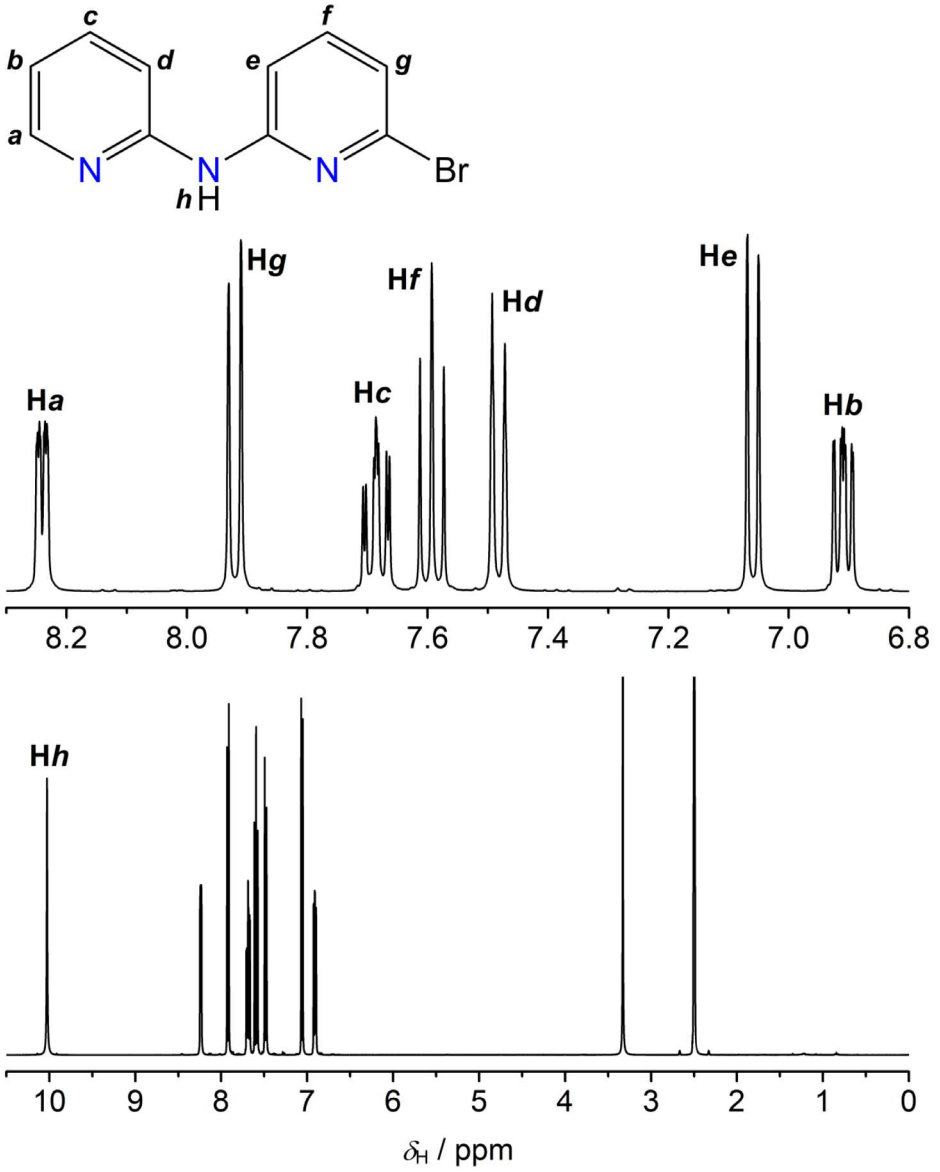

Supplementary Figure S1. Bottom: ^{1}H NMR spectrum of HBrdpa in DMSO-d_6 (298 K, 400.13 MHz). Top: atom-labelled structure of HBrdpa and magnification of the spectral region between 8.30 and 6.80 ppm. Processing parameters (TopSpin 4.0.6 [4]): SI = TD, LB = 0.30 Hz. δ_H (ppm) = 2.50 (quintet, residual protons in DMSO-d_6), 3.33 (s, water, OH).

(3) 2D NMR spectra of HFdpa

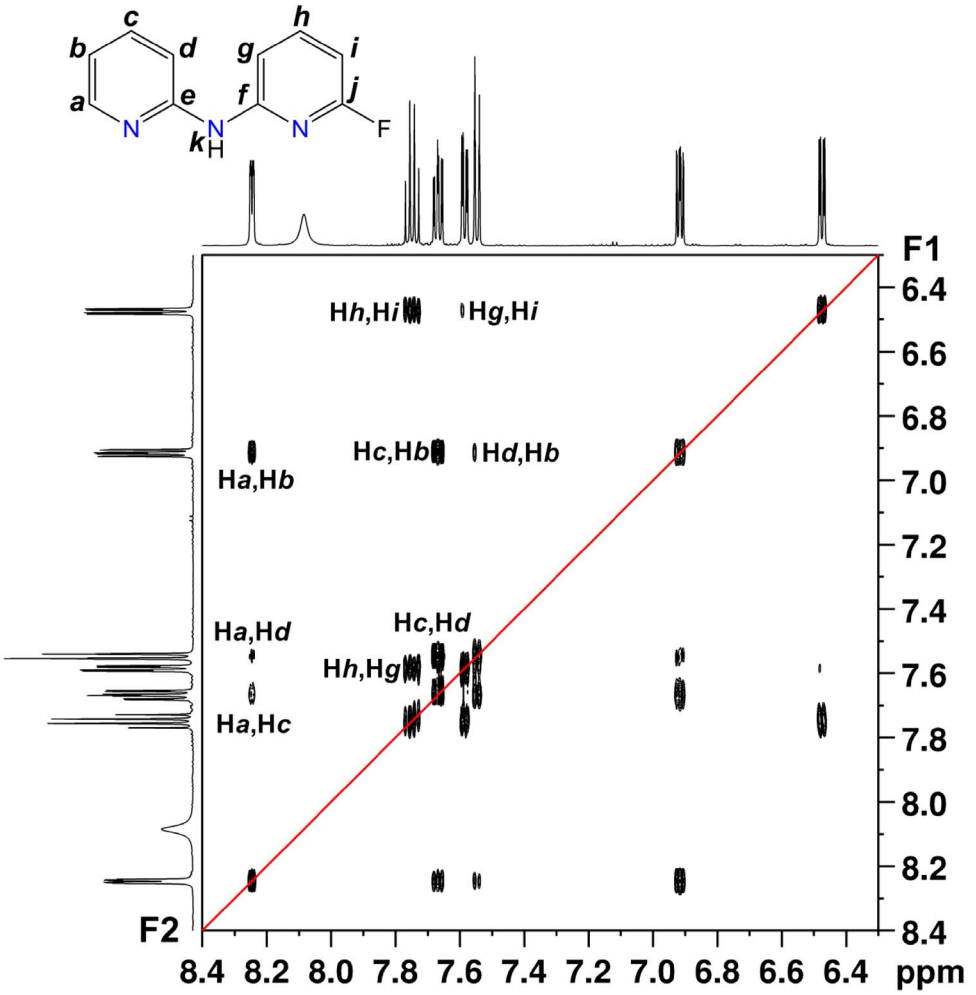

Supplementary Figure S2. Atom-labelled structure and ^{1}H–^{1}H COSY spectrum of HFdpa in CD_3CN between 8.40 and 6.30 ppm (298 K, 600.13 MHz). The labelling of the cross-peaks indicates the ^{1}H–^{1}H coupling (F2, F1). The red line highlights the diagonal peaks. Processing parameters (TopSpin 4.0.6 [4]) for F2 (*x* axis): SI = TD, LB = 1.00 Hz. Processing parameters for F1 (*y* axis): SI = 2·TD, LB = 0.30 Hz.

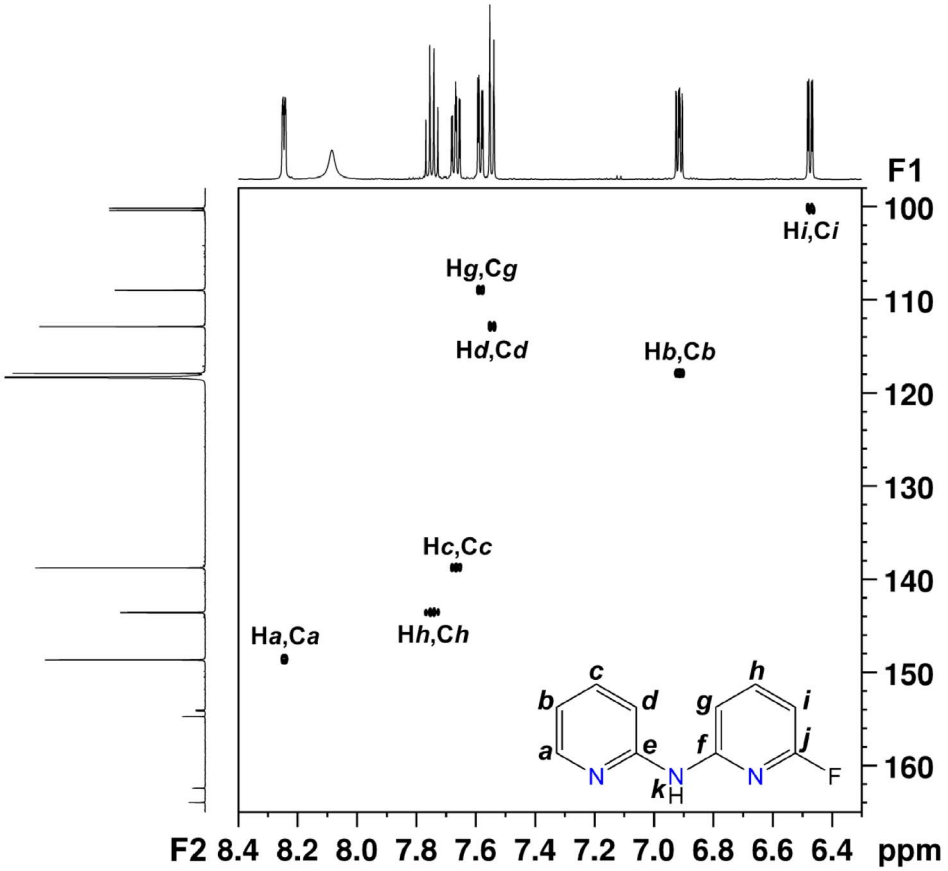

Supplementary Figure S3. Atom-labelled structure and ^{1}H–^{13}C HSQC spectrum of HFdpa in CD_3CN for δ_H = 8.40–6.30 ppm and δ_C = 165–98 ppm (298 K, 600.13 MHz for F2, 150.90 MHz for F1). The labelling of the cross-peaks indicates the ^{1}H–^{13}C coupling (F2, F1). Processing parameters (TopSpin 4.0.6 [4]) for F2 (*x* axis): SI = 2·TD, LB = 1.00 Hz. Processing parameters for F1 (*y* axis): SI = 3·TD, LB = 0.30 Hz.

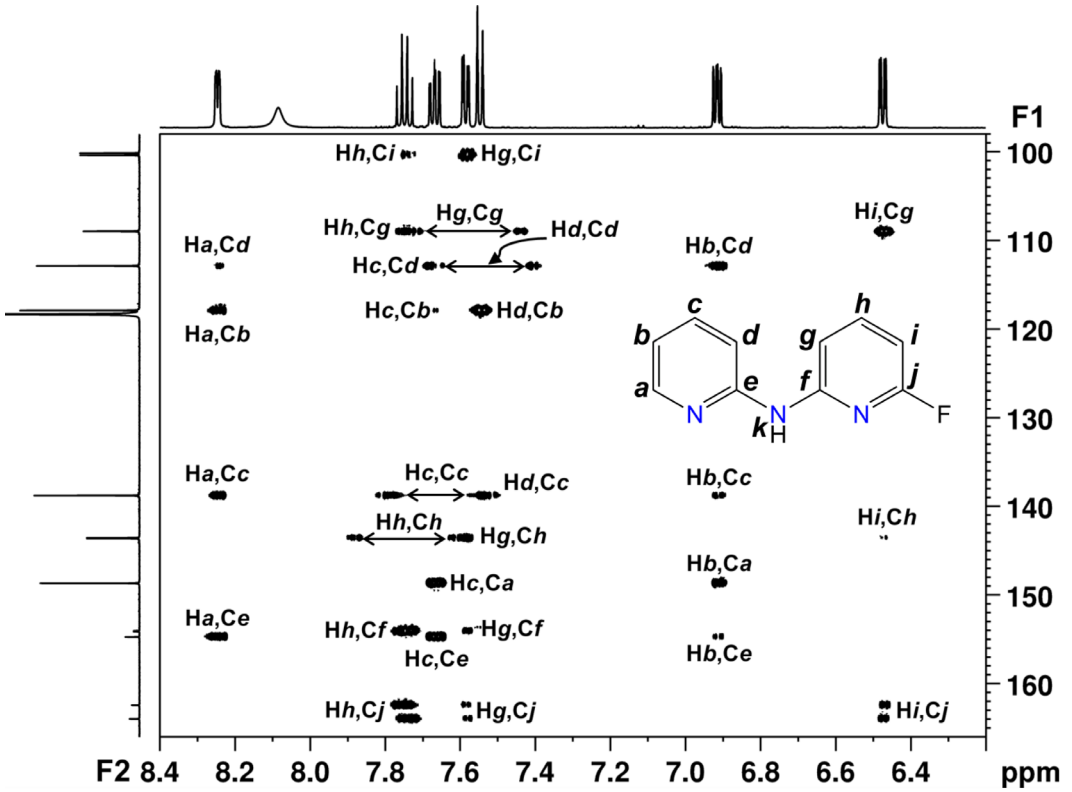

Supplementary Figure S4. Atom-labelled structure and ^{1}H–^{13}C HMBC spectrum of HFdpa in CD_3CN for δ_H = 8.40–6.30 ppm and δ_C = 166–98 ppm (298 K, 600.13 MHz for F2, 150.90 MHz for F1). The labelling of the cross-peaks indicates the ^{1}H–^{13}C coupling (F2, F1). Although a low-pass filter was employed for a better ^{1}J suppression (pulse program: hmbcetgpl3nd), the spectrum exhibits the remanence of ^{1}J couplings for sites *c*, *d*, *g*, and *h*. Processing parameters (TopSpin 4.0.6 [4]) for F2 (*x* axis): SI = TD, LB = 1.00 Hz. Processing parameters for F1 (*y* axis): SI = 3·TD, LB = 0.30 Hz.

(4) 2D NMR spectra of H_6tren(dpa)$_3$

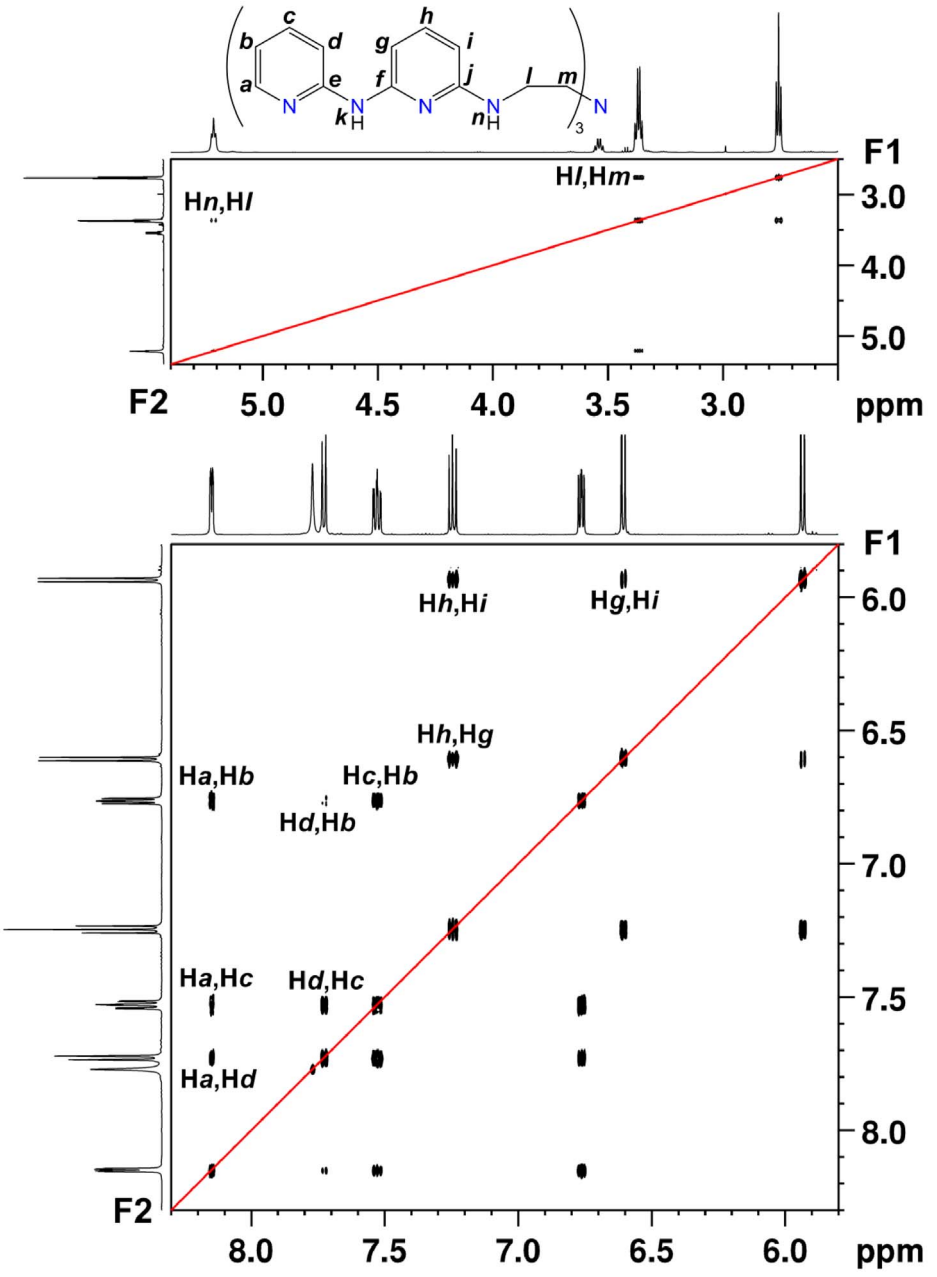

Supplementary Figure S5. Atom-labelled structure and ^{1}H–^{1}H COSY spectrum of H_6tren(dpa)$_3$ in CD_3CN for (bottom) δ_H = 8.30–5.80 ppm and (top) δ_H = 5.40–2.50 ppm (298 K, 600.13 MHz). The labelling of the cross-peaks indicates the ^{1}H–^{1}H coupling (F2, F1). The red line highlights the diagonal peaks. Processing parameters (TopSpin 4.0.6 [4]) for F2 (*x* axis): SI = TD, LB = 1.00 Hz. Processing parameters for F1 (*y* axis): SI = 2·TD, LB = 0.30 Hz.

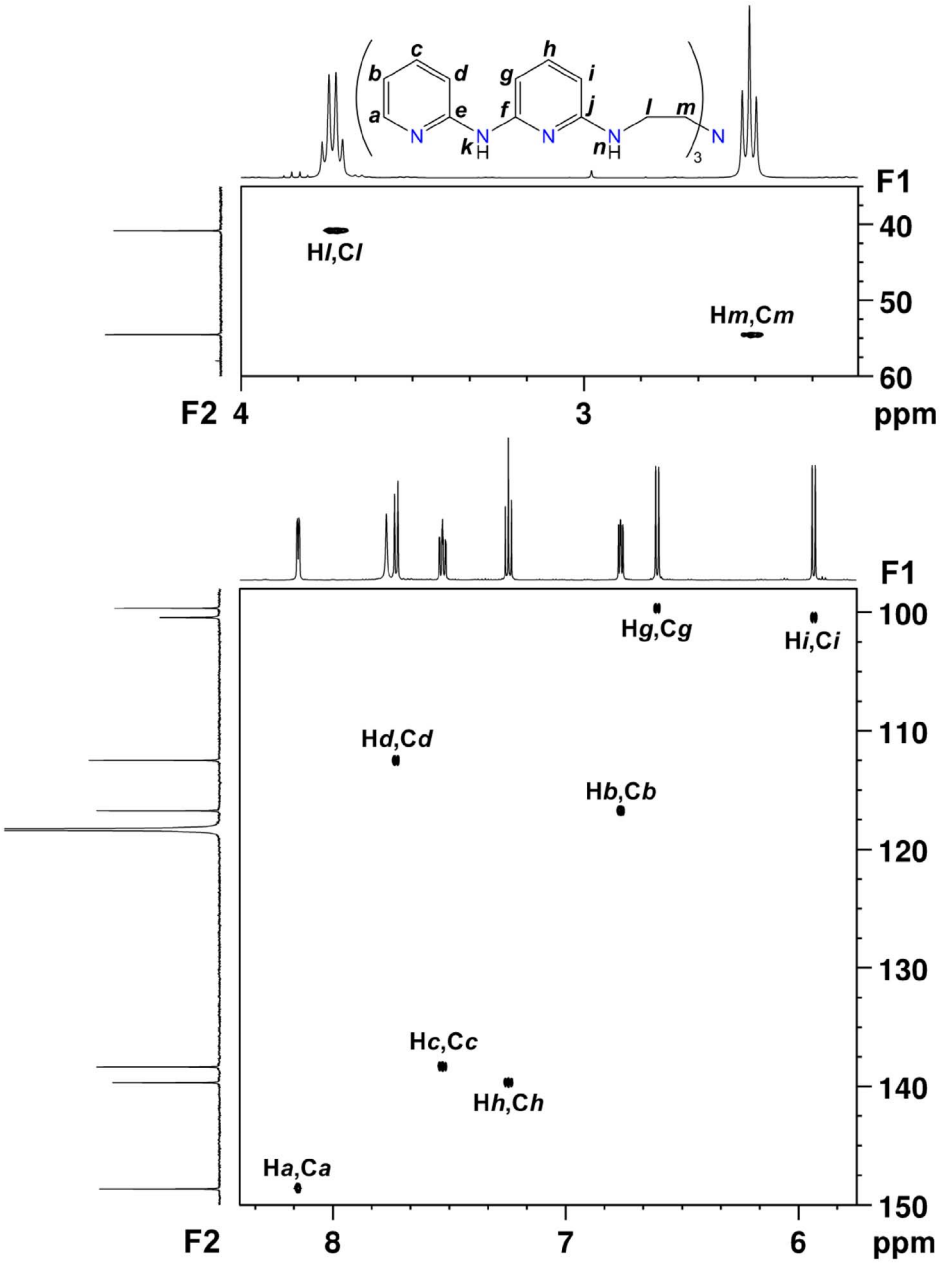

Supplementary Figure S6. Atom-labelled structure and ^{1}H–^{13}C HSQC spectrum of H_6tren(dpa)$_3$ in CD_3CN for (bottom) δ_H = 8.40–5.75 ppm, δ_C = 150–98 ppm, and (top) δ_H = 4.00–2.20 ppm, δ_C = 60–35 ppm (298 K, 600.13 MHz for F2, 150.90 MHz for F1). The labelling of the cross-peaks indicates the ^{1}H–^{13}C coupling (F2, F1). Processing parameters (TopSpin 4.0.6 [4]) for F2 (*x* axis): SI = 2·TD, LB = 1.00 Hz. Processing parameters for F1 (*y* axis): SI = 3·TD, LB = 0.30 Hz.

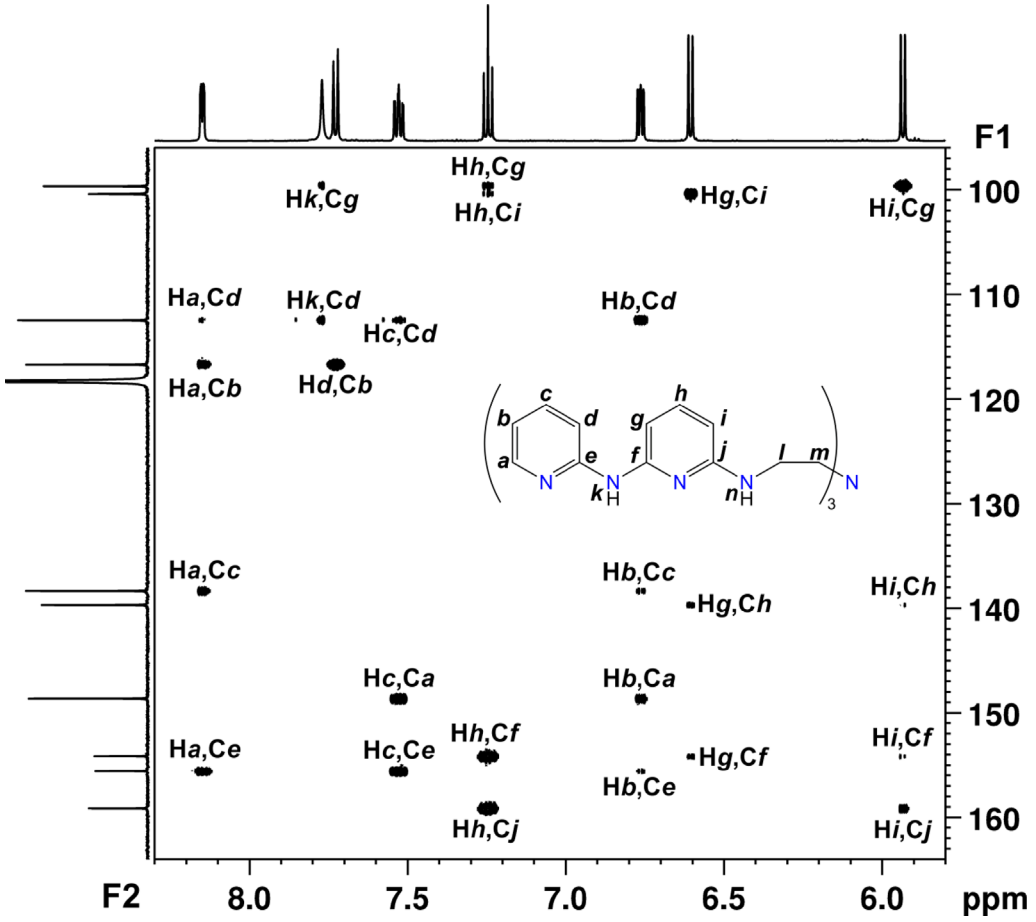

Supplementary Figure S7. Atom-labelled structure and ^{1}H–^{13}C HMBC spectrum of H_6tren(dpa)$_3$ in CD_3CN for δ_H = 8.30–5.80 ppm and δ_C = 164–96 ppm (298 K, 600.13 MHz for F2, 150.90 MHz for F1). The labelling of the cross-peaks indicates the ^{1}H–^{13}C coupling (F2, F1). Processing parameters (TopSpin 4.0.6 [4]) for F2 (*x* axis): SI = TD, LB = 1.00 Hz. Processing parameters for F1 (*y* axis): SI = 3·TD, LB = 0.30 Hz.

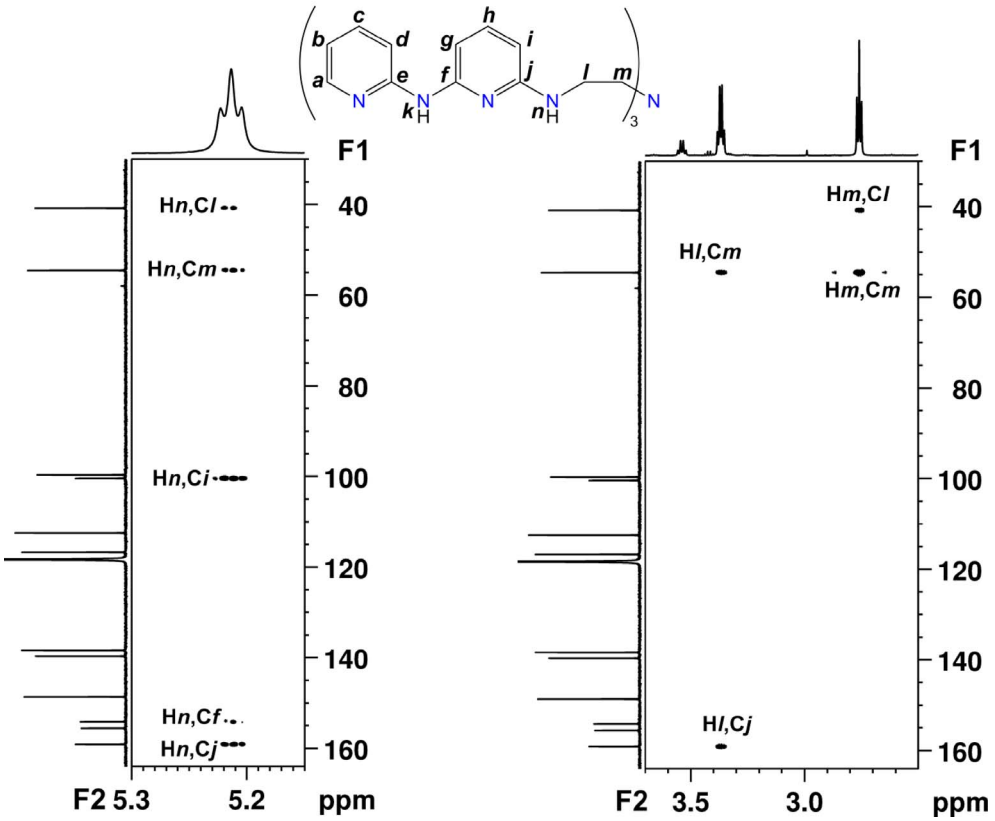

Supplementary Figure S8. Atom-labelled structure and ^{1}H–^{13}C HMBC spectrum of H_6tren(dpa)$_3$ in CD_3CN for (left) δ_H = 5.30–5.15 ppm, δ_C = 165–30 ppm, and (right) δ_H = 3.70–2.50 ppm, δ_C = 165–30 ppm (298 K, 600.13 MHz for F2, 150.90 MHz for F1). The labelling of the cross-peaks indicates the ^{1}H–^{13}C coupling (F2, F1). Although a low-pass filter was employed for a better ^{1}J suppression (pulse program: hmbcetgpl3nd), the spectrum exhibits the remanence of ^{1}J coupling for site *m*. Processing parameters (TopSpin 4.0.6 [4]) for F2 (*x* axis): SI = TD, LB = 1.00 Hz. Processing parameters for F1 (*y* axis): SI = 3·TD, LB = 0.30 Hz.

(5) Details on ^{1}H NMR and ESI-MS detection of SPa

After the reaction described in Scheme 3b, H_6tren(dpa)$_3$ was found admixed in a 1:0.26 MR with side-product **SPa**, which co-eluted during the FC purification. **SPa**, whose structure is represented in Scheme S2, arises from a further nucleophilic substitution reaction between H_6tren(dpa)$_3$ and BrHdpa. Due to its low symmetry, **SPa** introduces many extra peaks in the ^{1}H NMR spectrum of the chromatographed mixture (Figure S9). In particular, the spectrum shows a new set of eleven signals, indicated in Figure S9 by red circles, which are similar to those found in H_6tren(dpa)$_3$ in terms of hyperfine splitting and relative areas, and arise from the two "unmodified" branches of **SPa** (also colored in red in Scheme S2). The chemical shifts of seven of these signals are significantly different from those of H_6tren(dpa)$_3$, and they were easily identified in the ^{1}H NMR spectrum. On the other hand, the remaining four are hidden by the corresponding peaks of H_6tren(dpa)$_3$ (H*a*, H*b*, H*c* and H*h*). However, their presence was clearly demonstrated by 2D NMR spectroscopy analysis (^{1}H–^{1}H COSY). The branch of **SPa** undergoing the "extra" arylation (colored in blue in Scheme S2) should be responsible for a set of eighteen peaks. In Figure S9 seventeen over the eighteen expected peaks were detected (blue circles), and their presence was confirmed by ^{1}H–^{1}H COSY spectroscopy.

Unfortunately, due to the complexity of the spectra, the remaining peak was not spotted. This hidden signal is part of a set of sixteen peaks with identical areas, which arise from fourteen pyridyl and two amino protons. The fifteen spotted peaks are in the correct 1:2 integrated intensity ratio with the seven aromatic CH and two NH signals marked with red circles. The two remaining peaks correspond to the aliphatic H atoms and their integrated intensity is in fact in the expected 2:1 and 1:2 ratio with respect to the fifteen aromatic peaks (sixteen expected) and the aliphatic signals marked with red circles, respectively. All the aliphatic protons of **SPa** were assigned with good confidence, following the same scheme adopted for H_6tren(dpa)$_3$, while the assignment of the aromatic resonances is not straightforward due to many overlapping peaks. Therefore, the high-field region is the most informative one to understand which species are present in a sample, and to estimate their MR.

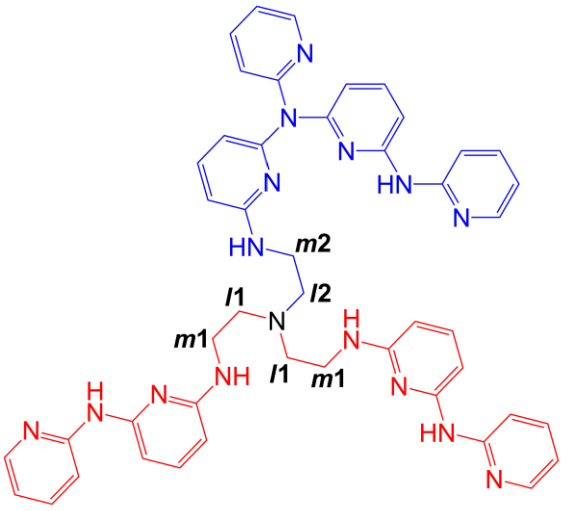

Scheme S2. Structure of **SPa** and assignment of the aliphatic H atoms. The red (blue) region of **SPa** generates the ^{1}H NMR signals marked with red (blue) circles in Figure S9 (below).

These NMR spectroscopy findings are in accordance with ESI-MS spectrometry measurements. The ESI-MS spectrum of the chromatographed mixture containing H_6tren(dpa)$_3$ and **SPa** is shown in Figure S10. Two intense and well resolved peaks are present at m/z = 654.4 (100%) and 823.5 (41%), which are well simulated by the ionic species $[H_6\text{tren(dpa)}_3 + H]^+$ and $[H_5\text{tren(dpa)}_4 + H]^+$ ([**SPa** + H]$^+$). The intensity ratio between these two signals (~1:0.4) is lower than the MR observed with ^{1}H NMR spectroscopy (1:0.26). A minority peak well simulated by $[H_4\text{tren(dpa)}_5 + H]^+$ is clearly visible at m/z = 992.5 (8%), even if the species H_4tren(dpa)$_5$ was not detected in the ^{1}H NMR spectrum of the same mixture. Since NMR is a better quantitative technique than ESI-MS spectrometry, these findings suggest that the signals related to $[H_5\text{tren(dpa)}_4+H]^+$ and $[H_4\text{tren(dpa)}_5+H]^+$ are enhanced here, probably due to ionic collision phenomena.

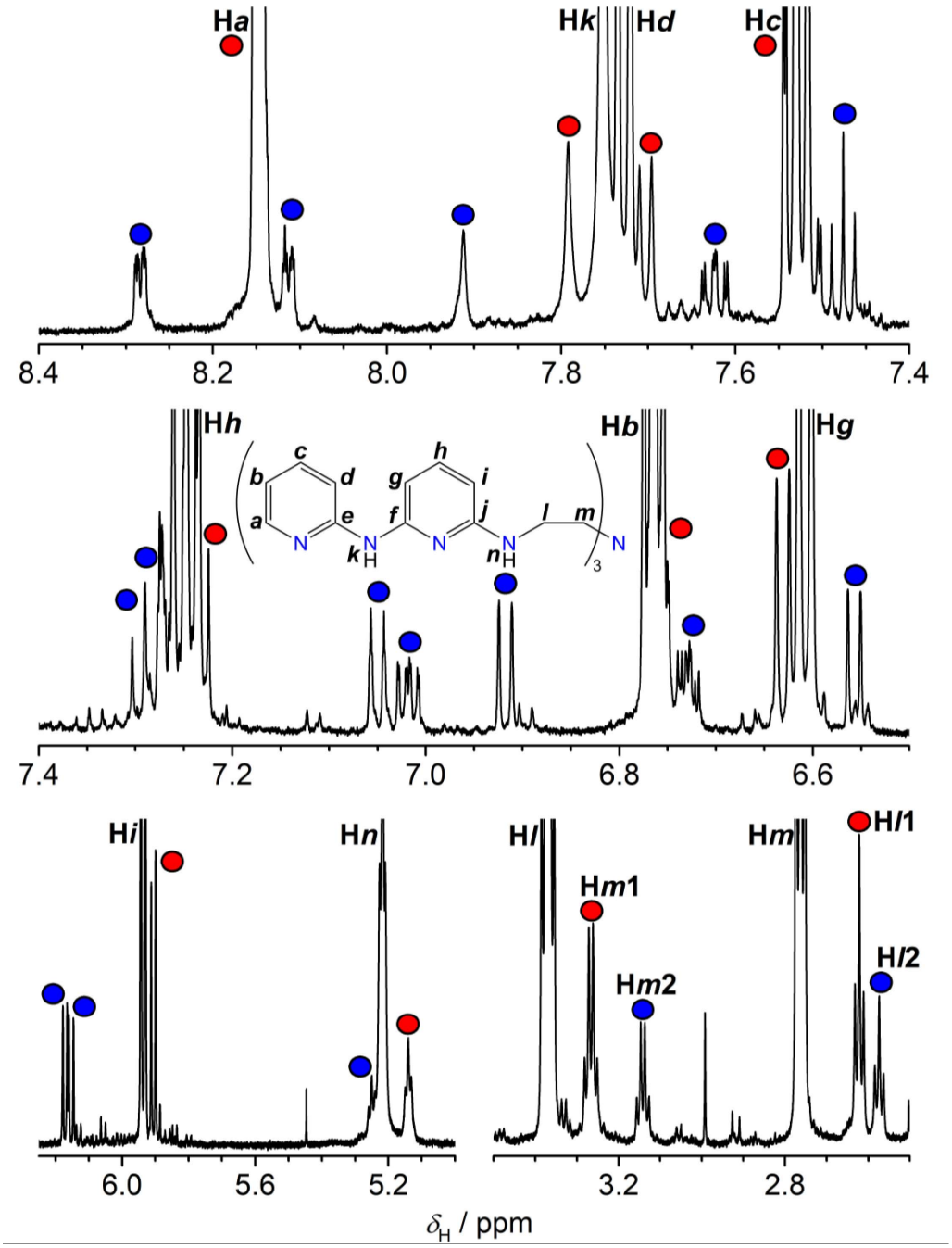

Supplementary Figure S9. ^{1}H NMR spectrum of the chromatographed mixture containing H_6tren(dpa)$_3$ and **SPa**, in CD_3CN, for (bottom right) δ_H = 3.50–2.50 ppm, (bottom left) δ_H = 6.25–5.00 ppm, (middle) δ_H = 7.40–6.50 ppm, and (top) δ_H = 8.40–7.40 ppm (298 K, 600.13 MHz). The labels show the assignments for H_6tren(dpa)$_3$ (all protons) and **SPa** (aliphatic protons only). The red and blue circles indicate the signals originating from the different branches of **SPa**, which are marked with the same colors in Scheme S2. Processing parameters (TopSpin 4.0.6 [4]): SI = TD, LB = 0.30 Hz.

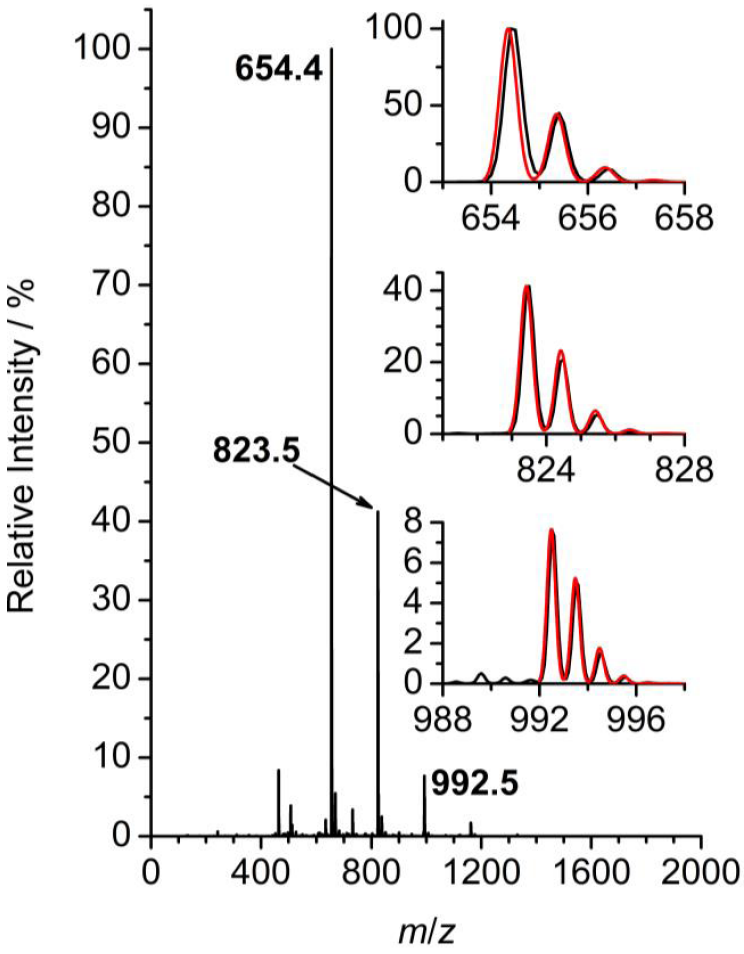

Supplementary Figure S10. ESI-MS spectrum of the chromatographed mixture containing H_6tren(dpa)$_3$ and **SPa** (direct infusion, CH_2Cl_2, positive ion mode). The insets show the experimental (black line) and simulated (red line) isotopic patterns of the peaks at m/z = 654.4 ([H_6tren(dpa)$_3$ + H]$^+$), 823.5 ([H_5tren(dpa)$_4$ + H]$^+$) and 992.5 ([H_4tren(dpa)$_5$ + H]$^+$). The peak at m/z = 464.3 (8%) was not assigned.

References

[1] S. J. Tereniak, R. K. Carlson, L. J. Clouston, V. G. Young, E. Bill, R. Maurice, Y.-S. Chen, H. J. Kim, L. Gagliardi, C. C. Lu, *J. Am. Chem. Soc.*, 2014, **136**, 1842-1855.

[2] S. Hohloch, J. R. Pankhurst, E. E. Jaekel, B. F. Parker, D. J. Lussier, M. E. Garner, C. H. Booth, J. B. Love, J. Arnold, *Dalton Trans.*, 2017, **46**, 11615-11625.

[3] Y.-J. Tsai, U. H. Lee, Q. Zhao, *Polyhedron*, 2017, **124**, 206-214.

[4] Bruker, *TopSpin 4.0.6*, Bruker AXS Inc., Madison, Wisconsin, USA, 2018.